JOURNAL OF SPACECRAFT AND ROCKETS
Vol. 46, No. 4, July–August 2009

Geometry of Fan Beam Albedo Measurements on Spin-Stabilized Satellites

Luc Fraiture*
64293 Darmstadt, Germany

DOI: 10.2514/1.41860

Because there is an imminent danger that most of the existing expert knowledge about attitude determination using fan beam albedo sensors on spin-stabilized satellites may become unavailable, it seems worthwhile to summarize this material in an archival paper. Toward this goal, all still-accessible reports and notes dealing with attitude reconstitution based on albedo slit sensors have been scrutinized. On this basis, we assessed the state of the art that was reached some decades ago; subsequently, no new satellite projects were realized that made use of this still-interesting type of attitude sensors. In the analysis of the available material, it appeared that attitude measurement stability and estimation accuracy still faced problems during particular time periods. In this context, elements have been identified that had been omitted from the ground-based attitude operations. These elements essentially concern the exclusion of specific measurement geometries, which, with certainty, invalidated certain measurements during time intervals of nonnegligible duration. The reported estimation concepts of the past have been updated not only on a theoretical basis, but also in light of more recent insights and operational experience gained from infrared sensing on spinning satellites. All this is included in a comprehensive and self-contained presentation based on the geometry of fan beam albedo sensing and its practical operational implementation.

Nomenclature

d	=	distance between the spacecraft and the Earth center, km
$\mathbf{E}$	=	nadir or Earth direction unit vector
i	=	inclination of the oblique fan beam at the satellite equator, rad
$\mathbf{N}$	=	spin-axis unit vector
R	=	Earth radius, km
$\mathbf{S}$	=	sun direction unit vector
α	=	sun–Earth dihedral angle around the spin axis, rad
β	=	nadir or Earth colatitude angle, rad
γ	=	angle between the sun and Earth direction, rad
ϵ	=	angular width of the observed illuminated crescent, rad
θ	=	sun direction colatitude, rad
ρ	=	radius of the apparent Earth disc, rad
τ	=	angle between the sun–Earth plane and spin-axis–Earth plane, rad
ϕ_0	=	half the apparent tangential extent of the lit Earth crescent, rad
ω	=	spin rate, rad/s

Introduction

FAN beam albedo attitude sensors were used on four satellites built in Europe before 1975. However, between 1975 and 1980 the number of new spin-stabilized spacecraft launches dramatically decreased in favor of projects relying on three-axis stabilization. One of the consequences of this relatively swift reorientation was that no resources were available to record the more advanced acquired knowledge of that time about the appealing properties of these sensors in publications with repository character. The projects referred to are the Highly Eccentric Orbit Satellite (HEOS) A1 (launched December 1968), HEOS A2 (January 1972), Cosmic Ray Satellite Version B (COS-B) (August 1975), and the European contribution to the International Sun-Earth Explorer Satellites (ISEE-B) (October 1977), for which the attitude hardware was the same as that of the COS-B (but the attitude estimation, together with most other ground operations, had been handed over to NASA). The bulk of attitude analysis work performed in the name of or by European Space Research Organisation (ESRO), the predecessor organization of ESA, in particular the work contained in a note by Massart for COS-B briefly referenced in the book edited by Wertz [1] (see pp. 178–179 and 213–216), is no longer accessible. This is also the case for numerous non-European references, which were cited concurrently by Wertz, none of which referred to albedo slit sensors. The geometrical descriptions in that book assumed that albedo attitude sensing was performed by telescopes with a narrow field of view (see [1], p. 173) and, thus, compared well with infrared pencil beams or horizon sensors, thereby neglecting the fact that the illuminated apparent Earth is seldom a circular disc. Further, the argument was made that the field-of-view geometry of a V-slit sun sensor is identical to a combination of two differently inclined albedo slit or fan beam sensors. The V-slit sun sensor data can be interpreted as being generated by the sun as a point source. This assumption is quite insufficient to deal with fan beam albedo sensors (FBAS) if we consider that the apogee of COS-B was at a height of 75,000 km, corresponding to an apparent Earth diameter of somewhat less than 10 deg.

The author of this paper had already compiled the essence of the geometrical insights related to FBAS in a working paper [2] published 1988 in preparation for a feasibility analysis. This analysis had to come to a conclusion concerning the compatibility of FBAS with the mission constraints defined for the four Cluster satellites. These spacecraft were launched as two separate satellite pairs into highly eccentric orbits [3] in July and August 2000 for the exploration of the remote terrestrial magnetosphere in a tetrahedron formation flight. The FBAS attitude coverage and covariance studies [4,5], applicable to the early design phase of Cluster, revealed that not so much the accuracy, but rather the sensor coverage (periods of availability of useful measurements) was insufficient to cope with the need to timely execute critical velocity increment maneuvers, each time requiring other spin-axis orientations achieved with prescribed precision. We were motivated on the one hand by the studies just mentioned, which uncovered gaps in the area of sensor coverage in past practice together with a suboptimal approach in the area of attitude estimation, and on the other hand by the absence of accessible and specific reference literature. In other words, the present paper aims to provide a comprehensive compilation of known but unpublished material, simplified in its trigonometric

Received 28 October 2008; revision received 15 March 2009; accepted for publication 7 April 2009.

*Lucasweg 6.

representation, complemented in the area of FBAS coverage aspects, and updated with guidelines for optimal attitude estimation. It will allow the reader to approach albedo fan beam sensing in an unbiased way, requiring only basic background knowledge. The information presented should further avoid the unwarranted discarding of a potential albedo sensor option due to the initial study costs for an initial assessment, comparison, and conception of attitude software and operations.

In the next section, we start by recalling the high-level arguments that speak for and against using albedo sensing on spin-stabilized satellites. Thereafter, we introduce the geometry applicable to Earth sensing on a spinning satellite and address basic generalities about the shape of the Earth albedo lunes (see [1], pp. 83–90). Before being able to explicitly formulate the measurement equations, we describe the different geometrical aspects of the time tagging (referred to hereafter as "datation") of the FBAS measurement events. This naturally leads to the measurement equations and, with them at our disposal, we give suggestions for robust short-term attitude determination and high-precision Gauss–Markov long-term attitude estimation in light of recently applied mathematical and operational insights. We conclude the paper by enumerating and detailing the coverage criteria, because they contain additional nontrivial trigonometrical problems that were not included in the ESA control center software, as mentioned earlier. We will systematically assume the availability of only one meridian and one inclined fan beam employed for sun and albedo sensing together.

Generalities About Albedo Attitude Sensing Adequacy

For Earth-bound spin-stabilized satellites for which the orbits evolve more or less beyond the radiation belts (operational altitudes normally well above 15,000 km), there are, apart from the sun, three competing classical sensing sources. They are 1) the weather and daytime insensitive infrared horizon (radiation wavelength near 16 μm), 2) the weather and surface texture sensitive as well as daytime dependent albedo (diffusely reflected sunlight), and, finally, 3) the stars.

The star sensors are also called star mappers or star scanners and are able to detect bright stars generally below visual magnitude five, according to today's flight-proven technology. The star catalogues for these sensors usually comprise much less than 500 stars. Most solar systems' planets are normally detected as well. The star mappers rely on fan beams (of limited size to prevent, as much as possible, simultaneous triggering on different stars), which succeed in collecting enough photons of an isolated star if the spin rate is low enough. Therefore, spin rates of 20 rpm can be considered to be at the limit of acceptability.

The very successful infrared pencil beam sensors operate from near Earth to some 65,000 km in altitude, where the intensity of Earth radiation of the good wavelength starts to become rather weak. These sensors operate in the range from 15 to 100 rpm. Fan beam infrared sensors exist as well (flown on SIRIO I, launched in 1977), but their space qualification in flight came too late for a breakthrough on the shrinking hardware market for spinning satellites. The time constants of the triggering electronics of the infrared sensors are normally tailored to the mission characteristics, which essentially are the mean operational altitude and the mean operational spin rate.

Finally, we have the albedo sensors. But albedo radiation of the lit part of the Earth is known to vary substantially over very short distances and is unstable over time. The cure to this problem is to only select this type of sensor for missions operating for longer times on altitudes higher than 50,000 km, where the apparent Earth disk becomes small enough to ensure that albedo variations at the Earth surface correspond to apparent angular sizes of lesser importance at the satellite. These favorable conditions were exploited by magnetospheric satellites on highly eccentric orbits as explained before. By tuning the triggering electronics, albedo sensors can operate with spin rates of less than 5 rpm up to any meaningful higher spin rate. The advantage of the fan beam over the telescope sensor is the widening of the coverage, which is essential for far-Earth missions. Furthermore, a fan beam allows for a smoother gradient of the collected radiation at the dark/lit and lit/dark transitions, improving the accuracy of triggering in the presence of local albedo discontinuities. Moreover, albedo sensor technology is cheap and one can reach three sigma accuracies [4,5] between 0.5 and 1.0 deg. (For example, COS-B refined attitude estimation reached [6] a precision of approximately 1.0 deg.) Another advantage of albedo sensors, in general, is their potential use as moon sensors. Also, by adapting the electronics, albedo and sun sensing can be combined into one and the same sensor (as was done for COS-B and ISEE-C).

To be complete, we have to say a word about magnetometers. This type of sensor is adequate for low Earth orbits typically below 1000 km, because only for such heights is the geomagnetic field stable and models accurate. Moreover, low perigee altitudes for satellites on highly eccentric orbits tend to heavily oscillate due to luni–solar perturbations. Consequently, magnetometers are not the right attitude sensors for attitude purposes in such missions, whereas, in contrast, albedo sensors are useful. Thus, if one goes for spin stabilization, and the spin rate for a far-Earth mission should be 20 rpm or higher, albedo sensing is often the only choice. Also, for low spin rates and attitude accuracy requirements of at most 0.5 deg, star mappers may be an overdesign.

Attitude and Illumination Geometry

When a satellite is passively spin stabilized, it is normally equipped with a nutation damper. As a consequence, outside attitude and orbit control maneuvering periods, the spin axis will be aligned with the inertially fixed angular momentum, which in turn is aligned with the largest principal moment of inertia of the spacecraft. Disturbing torques on far-Earth missions are essentially due to solar radiation pressure. Other disturbances only play a role if the perigee is low. Consequently, the spin-axis attitude drift is normally negligible within the time span of days and, in all that follows, we assume that the spin axis is an inertially fixed direction. This constancy is not necessarily available for the spin rate, which fluctuates under the influence of temperature variations of the spacecraft (variations of energy input and heat dissipation [7]). If we aim at high-attitude-estimation accuracies, the spin-rate variation must not be neglected in the translation of the spin-rate-dependent sensing events into angular measurements, which we will present in the section entitled "Measurement Equations." The spinning satellites we will consider are supposed to rely on sun and Earth sensing alone. This assumption leads to a few basics, which apply independently of the actual sensing principles and the hardware used. We assume that the sun and Earth unit vectors, **S** and **E**, are pointing from the spacecraft toward the sun or the Earth, respectively. We complement these vectors with the spin-axis unit vector, **N**. For the interpretation of the measurements, it is important to recall that the spin motion is a counterclockwise rotation around the positive spin axis. The angles connecting the corresponding points of these three vectors on the unit sphere centered in the satellite at the point A are as shown in Fig. 1. More specifically, we have the sun colatitude θ and the Earth colatitude β (both between zero and π), and the sun–Earth dihedral angle α (which varies between zero and 2π). All measurements will essentially be reduced directly or indirectly to these angles, which lead to the well-known basic equations

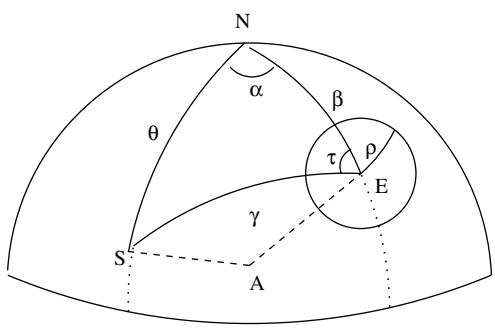

Fig. 1 Basic attitude triangle for the sun–Earth sensing combination.

$$(\mathbf{N}, \mathbf{S}) = \cos\theta \tag{1}$$

$$(\mathbf{N}, \mathbf{E}) = \cos\beta \tag{2}$$

$$(\mathbf{N}, (\mathbf{S} \times \mathbf{E})) = \sin\theta \sin\beta \sin\alpha \tag{3}$$

where (,) denotes a scalar product. These equations have been in use since the early days of satellite operations, as one can read in a note by Werking [8]. It is only gradually, from approximately 1975 onward, that the availability of independent measurements (in the sense that their covariance matrix had full rank) that could be simultaneously exploited in attitude estimation by these three equations was recognized to be substantially more accurate and numerically more stable than the use of the best choice of two equation types out of three. The older practice, if not dictated by the nature of the measurements themselves, was not only documented in Werking's note [7], but also in the study by Johansson [9] dealing with HEOS A2 attitude determination; it was further detailed in Chapter 11 of Wertz [1]. In this respect we may report that Massart had included the option of employing the combination of the three previous equations in the COS-B attitude software, whereas this author had implemented the operational attitude estimation software for the support of the low Earth spin-stabilized satellite ESRO IV launched in 1974, solely based on the simultaneous use of Eqs. (1–3). We hereafter always assume that modern sensing techniques admit the simultaneous application of Eqs. (1–3).

Neither θ nor β are direct linear functions of the basic measurements we will consider, in contrast to α, which happens when the apparent Earth is completely lit. It is assumed that the sun colatitude is available, and considerations will be limited to albedo sensing only. Nevertheless, we wish to warn the potential user of V-slit sensors against any emphasis put on bias determination, contrary to what is implicitly suggested in the book edited by Wertz [1] (see pp. 219–221), but to take the literal meaning of what is said in the Introduction of Chapter 14 of the same reference. Notwithstanding theoretical observability, we had to conclude in this particular case that the determination of *constant* sensor timing and alignment biases had to be quite accurate to not harm the actual estimation process as such. To perform this verification, a covariance analysis of the bias estimation has to be carried out in the presence of an available error-free attitude and realistic measurement inaccuracies. The expected *constant* bias estimation precision, logically, has to be much better than the (last-minute) calibrated prelaunch bias accuracy (normally verified on the launch pad). In this particular context, the compilation [10] of different related studies showed that this could normally not be achieved. This, by the way, was one of the facts that led to the information dilution theorem [11], which gave the theoretical basis confirming the observed difficulties.

Before coming back to more specific albedo-related technicalities, we first agree that an arbitrary line segment AB is denoted by an overbar $\overline{\mathrm{AB}}$ in contrast to an arc AB, which is denoted by a wide caret $\widehat{\mathrm{AB}}$. Also, (dihedral) angles are referred to by a caret spanning three characters. Furthermore, characters referring to points in a figure are never italicized.

We now observe that the illumination geometry of the Earth, seen by the spacecraft, depends only on the relative position of the satellite, the Earth center, and the sun direction. The scene under study is depicted in Fig. 2, which represents the plane defined by the Earth, sun, and satellite. The line $\overline{\mathrm{AO}}$ corresponds to the distance d of the spacecraft located at A to the center of the Earth at O. The Earth is assumed spherical with radius R. The vector $\mathbf{E}$ is along $\overline{\mathrm{AO}}$. The part of the Earth optically observable by the satellite is enclosed in a cone of semi-apex angle ρ. The apparent (arc) radius of the Earth disc is derived from $\sin\rho = R/d$. This view cone is in contact with the Earth at the (visibility) horizon, which corresponds to a small circle of radius $R\cos\rho$ passing through the points H and H′. The lit Earth horizon is called *the Earth limb*. The unit vector $\mathbf{S}$ and its oriented angle with $\mathbf{E}$ is denoted by $\tilde{\gamma}$. By oriented angle, we mean $0 \le \tilde{\gamma} < 2\pi$, starting with $\mathbf{S}$ and rotating counterclockwise around the vector product direction $(\mathbf{S} \times \mathbf{E})$. We propose to employ a coordinate system whose z axis is the inertial north direction. The oriented angle $\tilde{\gamma}$ and the nonoriented angle γ are then simply obtained from

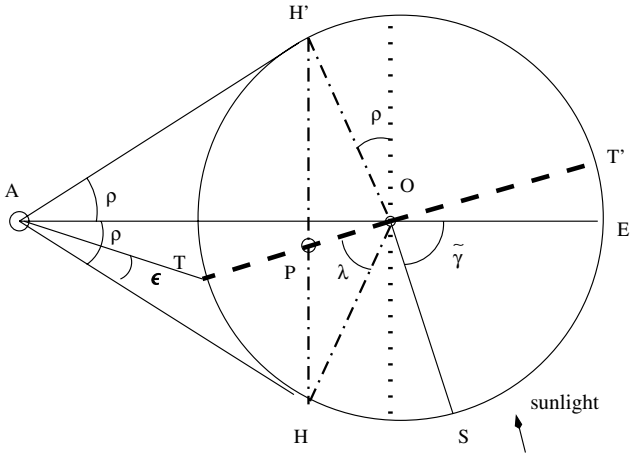

Fig. 2 Width ϵ of the illuminated lune in the satellite–sun–Earth plane.

$$\begin{aligned} \tilde{\gamma} &= \arg[\mathrm{sign}(\mathbf{S} \times \mathbf{E})_z \sqrt{(1 - (\mathbf{S}, \mathbf{E})^2}, (\mathbf{S}, \mathbf{E})] \\ \gamma &= \arccos(\mathbf{S}, \mathbf{E}) \end{aligned} \tag{4}$$

where the argument function $\arg(a, b)$ yields the angle ω with $0 \le \omega \le 2\pi$, assuming that $a = n\sin\omega$ and $b = n\cos\omega$ with $n = +\sqrt{a^2 + b^2}$.

Assuming the sun at infinity, the sun illuminates half the Earth, and the boundary of the lit hemisphere is the ideal *terminator*. This is an approximation neglecting the fact that the dark angle between the antisolar direction and the terminator is approximately 0.85 deg smaller than 90 deg due to the finite size of the sun and the refraction phenomena at dawn and dusk transitions. In Fig. 2, the terminator is the great circle passing through T and T′ on the sphere centered at O. The projection of the ideal terminator on a sphere centered at A has an elliptical shape, an arc of which can at most be approximated. The part of the lit Earth visible at A is that fraction of the lit hemisphere intruding into the view cone AHH′. Here, this is the sector bounded by TOH spanning the angle λ. Just by using γ and ρ, there are three questions we can now solve. First, what is the shape of the lit portion inside the apparent disk? Second, what is the value of the horizontal crescent width ϵ on a unit sphere centered at the spacecraft? And third, what is the size of the vertical crescent extension on the spacecraft unit sphere? The analytical quantification of the size of the albedo crescent by means of the solid angle spanned at A has, as far as we know, not been derived even today. Fortunately, this angle can be considered to be of negligible operational importance; hence, we will not deal with it.

By moving the line $\overline{\mathrm{OS}}$ clockwise in Fig. 2, while keeping $\overline{\mathrm{AE}}$ fixed, we see that the illumination of the apparent Earth starts when $\tilde{\gamma} = \rho$ and ends when $\tilde{\gamma} = 2\pi - \rho$. In detail, we differentiate between:

$$0 < \lambda \le \pi/2 - \rho \quad \text{when } \rho < \tilde{\gamma} \le \pi/2 \tag{a}$$

$$\pi/2 - \rho < \lambda \le \pi - 2\rho \quad \text{when } \pi/2 < \tilde{\gamma} \le \pi - \rho \tag{b}$$

$$\lambda = \pi - 2\rho \quad \text{when } \pi - \rho < \tilde{\gamma} \le \pi + \rho \tag{c}$$

$$\pi/2 - \rho \le \lambda < \pi - 2\rho \quad \text{when } \pi + \rho < \tilde{\gamma} \le 3\pi/2 \tag{d}$$

$$0 < \lambda \le \pi/2 - \rho \quad \text{when } 3\pi/2 < \tilde{\gamma} \le 2\pi - \rho \tag{e}$$

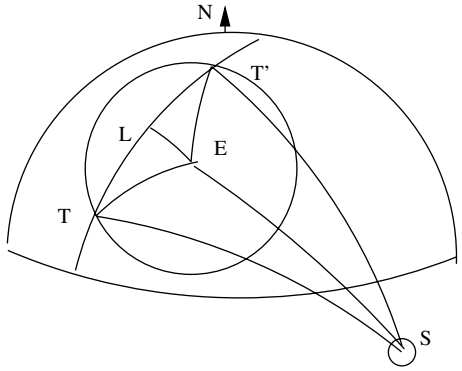

Fig. 3 Geometry of the Earth lune seen from the satellite.

With condition a, we have a concave D-shaped crescent, which becomes a convex or gibbous lune when b is satisfied, ending in full illumination of the apparent disk with condition c. The crescents with conditions d and e are the C-shaped mirror images of b and a, respectively.

The actual value of the angle λ, except in the case of full illumination, is obtained by subtracting the angle $\widehat{\mathrm{AOT}} = \pi/2 - \gamma$ from $\widehat{\mathrm{AOH}} = \pi/2 - \rho$, or $\lambda = \gamma - \rho$. To derive ϵ, we consider the triangle ATO, in which we have

$$\overline{\mathrm{AT}} \sin(\rho - \epsilon) = R \cos(\rho + \lambda) \tag{5}$$

$$\overline{\mathrm{AT}} \cos(\rho - \epsilon) = d - R \sin(\rho + \lambda) \tag{6}$$

which directly leads to

$$\tan(\rho - \epsilon) = \frac{\sin\rho \cos\gamma}{1 - \sin\rho \sin\gamma} \tag{7}$$

Next, we are interested in the extension ϕ_0 of the crescent above and below the satellite–Earth–sun plane, because we need it for coverage considerations. The actual geometry is represented in Fig. 3. There, the great circle passing through T and T′ approximates the terminator at 90 deg from the sun vector. Consequently, we have $\widehat{\mathrm{TS}} = \widehat{\mathrm{T'S}} = \pi/2$ and $\widehat{\mathrm{TE}} = \widehat{\mathrm{T'E}} = \rho$ as well as $\widehat{\mathrm{TT'}} = 2\phi_0$. We now consider the triangle ELT and note that $\widehat{\mathrm{EL}}$ is equal to $\pm(\pi/2 - \gamma)$, depending on whether γ is smaller or larger than $\pi/2$, and is perpendicular to $\widehat{\mathrm{TT'}}$. Moreover, because ELT is a rectangular spherical triangle, we find that

$$\cos\rho = \sin\gamma \cos\phi_0 \tag{8}$$

by applying the cosine rule. Note that T and T′ define a great circle uniquely, and this circle does normally not comprise E, except if $(\mathbf{E}, \mathbf{S}) = 0$.

V-Slit Sensor

In Fig. 4, we display the geometry of a meridian fan beam, for which the field of view extends over an arc from D to E, and a skew fan beam, for which the arc length is $\widehat{\mathrm{AB}}$. We will explicitly use neither the field-of-view lengths, nor the fact that these lengths are usually equal for the meridian and skew slit. Also, the assumption that the intersection of the optical field of view of the meridian and skew fan beams (if combined in one sensor) is occurring in the middle of the slits (which are physically not intersecting) plays no role in the trigonometrical relations we will derive. The combination of a meridian and a skew or inclined slit is normally called a V beam or V-slit sensor. The angle μ, which represents the declination of the field-of-view intersection with respect to the spacecraft equator, and the inclination angle c of the skew slit at the intersection are the quantities usually provided by the hardware manufacturers. For computational purposes, they are best replaced by the angles i and ζ

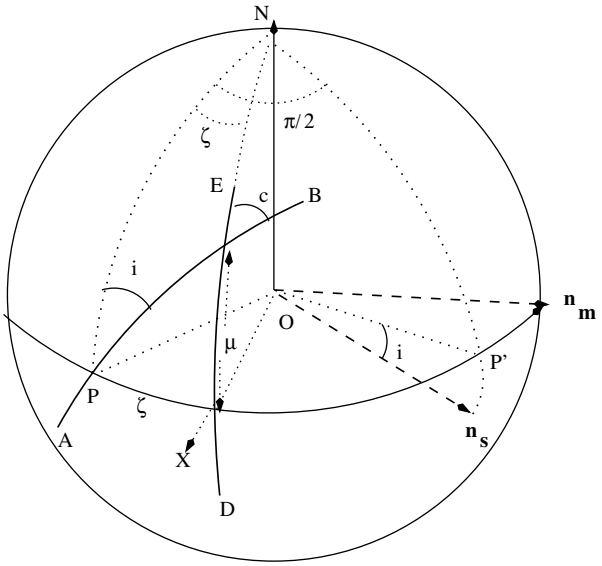

Fig. 4 Fan beam geometry on the unit sphere.

defined at the spacecraft equator. To that end, we use the following equations:

$$\sin i = \cos\mu \sin c, \qquad \tan\zeta = \sin\mu \tan c \tag{9}$$

The actual sensor output of the fan beam is a triggering and a corresponding time tag or datation upon the electrical detection of a positive or negative step in observed visible light intensity. This corresponds either to the entrance or exit of the slit into or out of the lit Earth (somewhere in the field of view), which can be an Earth limb as well as the terminator. The physical terminator is not only known to be a badly defined fuzzy area of low luminosity, but also the ideal geometrical terminator observed by the satellite is neither an arc of a great or a small circle. On top of all this, the horns of a crescent are on the side of the terminator if the Earth lune is concave. Therefore, the terminator completely disqualifies as valid reference, and we have to make sure to only deal with the limb. On COS-B, we had to uplink the choice of pulse sign to select the limb. In this way, the burden of the decision was left to coverage prediction; otherwise, we should have had to eliminate the undesirable pulses in a preprocessing. It may nevertheless be worthwhile to get both limb pulses if the spacecraft is more or less between the sun and Earth and we face "full Earth" (phase c), because this yields a supplementary independent measurement that will improve accuracy.

Measurement Equations

The nature of the sensing translates easily into geometry, provided we represent the physical slit by the normal to the corresponding great circle on the satellite centered unit sphere. At this point, we have to introduce a convention. In agreement with past applications, we assume that the x-body axis coincides with the line from the center O to the meridian slit on the spacecraft equator. The normal to the great circle containing the field-of-view arc from the meridian fan beam is then $\mathbf{n}'_{\mathbf{m}} = |0, 1, 0|$, where the accent denotes transposition. In this way, we have implicitly introduced a body reference system with the orthonormal base vectors $\mathbf{b_x}$ in the plane of $\mathbf{N}$ and the meridian slit; further, $\mathbf{b_z} = \mathbf{N}$ and, to complete the base, $\mathbf{b_y} = \mathbf{b_z} \times \mathbf{b_x}$. To obtain the normal to the inclined slit, we take the line $\overline{\mathrm{OP}}$ in Fig. 4, which in this particular figure has the coordinates $(\cos\zeta_0, -\sin\zeta_0)$ in the equator plane. This line is first rotated 90 deg counterclockwise, before being rotated further in the plane containing the spin axis and $\overline{\mathrm{OP'}}$ by the same angle in the same direction as the inclination of the slit at the equator. In Fig. 4, this yields $\mathbf{n}'_{\mathbf{s}} = |\sin\zeta_0 \cos i, \cos\zeta_0 \cos i, -\sin i|$.

We further introduce a "pseudoinertial" reference system as follows:

$$\mathbf{i}_x = \mathbf{i}_y \times \mathbf{i}_z = \frac{\mathbf{S} - \cos\theta\mathbf{N}}{\sin\theta}, \qquad \mathbf{i}_y = \frac{\mathbf{N}\times\mathbf{S}}{\sin\theta}, \qquad \mathbf{i}_z = \mathbf{N} \quad (10)$$

This is a reference system that varies with the slowly varying direction of the sun, as observed by a spacecraft on its orbit. With both coordinate systems at hand, we can represent the motion of the slit normals as functions of the time t and spin rate ω. The agreed (normally hardwired) time origin for a full spacecraft rotation is the crossing of the sun by the meridian slit. Hence, all sensor mountings have to refer to this origin, fixed by convention. For the position of the normal to the meridian slit as a function of time in the pseudoinertial system, we write

$$\mathbf{n}_m(t_m) = \begin{pmatrix} \cos(\pi/2 + \omega t_m) \\ \sin(\pi/2 + \omega t_m) \\ 0 \end{pmatrix} = \begin{pmatrix} -\sin(\omega t_m) \\ \cos(\omega t_m) \\ 0 \end{pmatrix} \quad (11)$$

and, for the normal to the skew slit, we obtain

$$\mathbf{n}_s(t_s) = \begin{pmatrix} -\sin(\omega t_s - \zeta_0)\cos i \\ \cos(\omega t_s - \zeta_0)\cos i \\ -\sin i \end{pmatrix} \quad (12)$$

The condition of tangency of the slit to the Earth horizon is now given by

$$(\mathbf{n}, \mathbf{E}) = \cos(\pi/2 \pm \rho) = \mp\sin\rho \quad (13)$$

where $\mathbf{n}$ stands for either normal to the skew or meridian slit. According to the rotation convention, the slit will touch the horizon and enter the Earth when the Earth center is only $\pi/2 - \rho$ apart from the normal and will leave the Earth when its center is already $\pi/2 + \rho$ away from the normal. Consequently, the lower sign corresponds to the space/Earth horizon crossing and the upper sign to the Earth/space horizon crossing. In principle no (eclipse), one (phases a, b, d, and e), or both horizon contact points can be lit. The components of $\mathbf{E}$ in the pseudoinertial system are

$$e_x = \frac{\cos\gamma - \cos\theta\cos\beta}{\sin\theta}, \qquad e_y = \frac{(\mathbf{N}, \mathbf{S}\times\mathbf{E})}{\sin\theta}, \qquad e_z = \cos\beta \quad (14)$$

not forgetting that these components and the angle ρ are functions of absolute time. Substituting Eqs. (11) and (14) into Eq. (13) yields

$$\pm\sin\rho\sin\theta = [\cos\gamma - \cos\theta(\mathbf{E}, \mathbf{N})]\sin(\omega t_{m\pm}) - (\mathbf{N}, \mathbf{S}\times\mathbf{E})\cos(\omega t_{m\pm}) \quad (15)$$

Henceforth, we will abbreviate $\omega t_{m\pm}$ by $\Omega_\pm^{(m)}$ and $(\omega t_{s\pm} - \zeta_0)$ by $\Omega_\pm^{(s)}$. Further, substituting Eqs. (12) and (14) into Eq. (13) yields the equation describing the functional relation between the skew slit tangency time and the attitude, namely,

$$\pm\sin\rho\sin\theta = [\cos\gamma - \cos\theta(\mathbf{N}, \mathbf{E})]\cos i\sin(\Omega_\pm^{(s)}) - \cos i\cos(\Omega_\pm^{(s)})(\mathbf{N}, \mathbf{S}\times\mathbf{E}) - \sin\theta\sin i(\mathbf{N}, \mathbf{E}) \quad (16)$$

There is one more equation that applies if the apparent Earth is fully lit, because then we also measure the angle 2κ, swept out by the meridian slit from Earth entrance T_a to Earth exit T_b, as shown in Fig. 5. This angle can be found from

$$\sin\kappa = \sin\rho/\sin\beta \quad (17)$$

However, Eq. (17) does not uniquely define $0 \le \beta \le \pi$ and is thus not very useful for estimation. Moreover, when we have "full Earth," Eq. (15) [and also Eq. (16)] is available in the "plus" and "minus" version, which represents the same information as Eq. (17). But Eq. (17) may nevertheless be interesting for simulation and coverage prediction calculation, because the angle α displayed in Fig. 1 and employed in Eq. (3) can now be composed as follows:

$$\alpha = \Omega_\pm^{(m)} \mp \kappa \quad (18)$$

which allows the transformation of Eq. (3) in the following way:

$$(\mathbf{N}, \mathbf{S}\times\mathbf{E}) = \sin\theta\sin\beta\sin(\Omega_\pm^{(m)} \mp \kappa) = \sin\theta[\sqrt{\cos^2\rho - \cos^2\beta}\sin(\Omega_\pm^{(m)}) \mp \sin\rho\cos(\Omega_\pm^{(m)})] \quad (19)$$

We terminate this section by noting that the concept of geometrically defining the tangency time tag in the way just outlined was already employed for the HEOS satellite software, but corresponding reports were disposed of or can no longer be traced back.

Attitude Estimation

Basically, attitude estimation in an operational context is not only the mere derivation of a result in the presence of random errors, but is equally a sampling strategy and method selection to cope with such things as temporary unavailability or loss of attitude knowledge and best estimation accuracy requirements. For the former problem, we need a quick and *robust attitude determination*, but not necessarily an accurate method to be applied as soon as usable measurement data have been acquired. To satisfy demanding precision requirements, a batch *optimal attitude estimation* for which the availability of results is not time critical can be applied, relying on reasonable initial parameters. We should not forget that an accurate spin-axis attitude is normally not required during an attitude slew, but the monitoring of a slew may ask for the support by a quick robust scheme, assuming a reduced precision. In the usual case, when payloads are operational, the attitude is constant and, in that case, it is consequently not necessary to foresee a (near) real-time attitude estimation update.

Another aspect that is typical for spin-stabilized satellites relying on Earth sensing is the continuous change all over the orbit of the configuration consisting of sun and Earth directions relative to the spacecraft. This has two main consequences. One is the natural change of achievable estimation precision in the presence of constant accuracy performance of measurement devices. This can be inferred from the value of the determinant of the coefficients of the equation system comprising Eqs. (1–3), which is equal to $\sin^2\gamma$. Consequently, this system of equations becomes singular when γ approaches zero. Based on existing practice, we suggest not using the data from intervals during which the value of γ is less than 15 deg. The influence of the geometrical configuration on attitude accuracy can be exploited by choosing a particular data interval to perform an optimal attitude estimation, whereas, in contrast, the robust short-term attitude determination cannot wait for the best configuration. The other of the two main consequences is the smooth change of the ideal measurements over time. This physically smooth evolution allows the implementation of smoothing of the real measurements, which enables us to substantially reduce the random noise input. Both features were successfully implemented in recent operations making use of infrared pencil beams, for which estimation accuracy could be improved by almost an order of magnitude [12,13].

For the robust attitude determination, we first assume that we have a reliable value for the sun colatitude in the form of $\cos\theta$ and, thus, equally $\sin\theta = +\sqrt{1 - \cos^2\theta}$. We will use this knowledge in Eqs. (15) and (16); because ρ and γ are also available quantities, Eqs. (15) and (16) can be reduced to the form

$$a_1(\mathbf{E}, \mathbf{N}) + b_1(\mathbf{N}, \mathbf{S}\times\mathbf{E}) = p_1 \quad (20)$$

$$a_2(\mathbf{E}, \mathbf{N}) + b_2(\mathbf{N}, \mathbf{S}\times\mathbf{E}) = p_2 \quad (21)$$

where we do not care about the fact that the coefficients contain measurements. In practice, if the FBAS has coverage of a lit fraction of the Earth, we will have two such equations at our disposal for only one of the space/Earth or Earth/space transitions of both the meridian and skew slit. If there is no skew slit, we end up with ambiguities that we do not address here. The system of equations thus determines the unknowns $(\mathbf{E}, \mathbf{N})$ and $(\mathbf{N}, \mathbf{S}\times\mathbf{E})$, and these values provide the right-hand-side members of Eqs. (2) and (3), whereas Eq. (1) is available by assumption. By disregarding the normalization constraint for $\mathbf{N}$, we thus have to resolve two linear systems of equations in cascade.

This rudimentary method can (and should) be refined by first making a smoothing of the transition time measurements over some minutes; subsequently, after having obtained the unconstrained **N**, we can repeat the resolution of the system equations (1–3) by applying the normality constraint.

For the optimal attitude estimation, we propose to solve a Gauss–Markov system, which implies the separation of measurements and unknowns in the separate sides of the equations. To this aim, we propose to use "intermediate variables" introduced and tested successfully as described in a recent paper [14]. This method consists of creating a number of unknowns, which is just sufficient to get rid of measurements in the equations that contain the original or essential unknowns, which in our case are the two parameters x_1 and x_2 defining **N** uniquely (e.g., right ascension and declination). To achieve this goal, we add these new unknowns in trivial measurement equations containing the measurements equated to the new unknowns, called intermediate variables. The price we may have to pay is the potential generation of constraint equations, requiring a careful budgeting of their number and mutual independence to avoid the creation of an overdetermined singular system. We further propose to adhere to the principle of controlled correlation [12], which requires that, for a single optimal attitude determination, one employs, if possible, one smoothed measurement of each type selected independently at the epochs corresponding to the best configuration accuracy. The purpose of this approach is to minimize the influence of measurement biases on the outcome of the estimate, but it implies at the same time that random errors have been reduced below the assumed bias error level by smoothing each separate measurement type. In this case, we have either four different limb tangency time tags, provided we have at our disposal (potentially different) coverage periods for which the space/Earth and Earth/space relative tangency times have been recorded, or, if not, we must at least have two such measurements. Without loss of generality we assume that we only have one tangency type and, consequently, only two intermediate variables, $x_{m\pm}$ and $x_{s\pm}$, both denoting the angles swept out by the spinning spacecraft from the sun pulse occurrence to the limb transition occurrence of the meridian and the skew slit. The system of measurement equations is then

$$(\mathbf{N}(x_1, x_2), \mathbf{S}_0) = \cos\theta_0 \tag{22}$$

$$x_{m\pm} = \omega t_{m\pm} \tag{23}$$

$$x_{s\pm} = \omega t_{s\pm} \tag{24}$$

together with the adaptation of Eq. (15):

$$\begin{aligned}&\frac{1}{\sqrt{1-(\mathbf{S_m}, \mathbf{N}(x_1, x_2))^2}}\\ &\quad\times\{[\cos\gamma_m - (\mathbf{S_m}, \mathbf{N}(x_1, x_2))(\mathbf{E_m}, \mathbf{N}(x_1, x_2))]\sin(x_{m\pm})\\ &\quad-(\mathbf{N}(x_1, x_2), \mathbf{S_m}\times\mathbf{E_m})\cos(x_{m\pm})\} = \pm\sin\rho_m\end{aligned} \tag{25}$$

and of Eq. (16), namely,

$$\begin{aligned}&\frac{1}{\sqrt{1-(\mathbf{S_s}, \mathbf{N}(x_1, x_2))^2}}\\ &\quad\times\{[\cos\gamma_s - (\mathbf{S_s}, \mathbf{N}(x_1, x_2))(\mathbf{E_s}, \mathbf{N}(x_1, x_2))]\cos i\sin(x_{s\pm})\\ &\quad-(\mathbf{N}(x_1, x_2), \mathbf{S_s}\times\mathbf{E_s})\cos i\cos(x_{m\pm})\} - \sin i(\mathbf{N_s}, \mathbf{E_s})\\ &\quad= \pm\sin\rho_s\end{aligned} \tag{26}$$

altogether comprising the unknowns x_1, x_2 and x_{m+}, x_{s+} and/or x_{m-}, and x_{s-}. The subscripts of **S**, **E**, γ, and ρ are added to indicate that the epoch applicable to these quantities shall be consistent inside one equation, but, of course, need not be consistent among different equations. We can consider both Eqs. (25) and (26) to be constraint equations, that is, the values of ρ are perfect. However, it is certainly simpler and theoretically better to avoid the generation of constraint equations and to consider these angles as random values and add the corresponding variances in the covariance matrix needed to derive the optimal estimate. The advantage of intermediate variables is not only hidden in the potential to trivially obtain a canonical Gauss–Markov system of measurement equations, but also, due to the necessary increase of the dimension of the covariance matrix, a formally better differentiation and distribution of the information on the error sources is achieved.

Albedo Sensing Coverage Prediction

Producing a coverage prediction time list is an important operational task that is seldom addressed on its own in the literature, because it is the verification of a number of almost evident conditions that decide where and when we can expect useful measurements on the basis of a known approximate attitude and an orbit at a given calendar time. This time also corresponds to precise sun and moon positions. The most common example of a coverage problem is the collinearity of sun and Earth direction, leading to poor attitude estimates performed in that neighborhood. A more albedo-specific problem may be due to the moon, which can give rise to an unexpected triggering and disturb a triggering selection algorithm on board. Such events also need to be checked for infrared telescope sensors on spin-stabilized satellites in geostationary transfer orbits, with which the author assisted in the predicted detection of the moon more than once. The more critical interference of the moon occurs when it enters the fan beam field of view very close to the point of lit limb tangency, normally making the corresponding series of measurements useless for some time. On the other hand, an identifiable isolated moon triggering (depending on the preset triggering level of the sensor, taking into account that the geometrical albedo of the moon is 5.3 times weaker, in the mean, than Earth's albedo) may be a welcome, accurate, supplementary measurement.

We now provide a coverage checklist, giving coverage conditions that have to be verified at predefined time steps. Each separate coverage condition can be assorted with a different safety margin, σ, due to the inaccuracy of the attitude we are working with or to the operational specifications (e.g., sun blinding). If we ask a question that has to be answered by "no," the conclusion is "no coverage," and the checks have to be resumed at the start after making a time step.

Are we sufficiently remote from sun–Earth collinearity or is 15 deg $+\sigma < \gamma <$ 165 deg $-\sigma$, where σ should logically be a function of ρ?

Is the complete apparent Earth disk fully inside the field of view scanned by the fan beam? This question was not considered in the past and requires that

$$-\pi/2 < \xi_s^{\min} + \rho + \sigma < \pi/2 - \beta < \xi_s^{\max} - \rho - \sigma$$

is satisfied. In this inequality, $\xi_s^{\min}(<0)$ and $\xi_s^{\max}$ are the lowest and highest declinations of the skew slit field of view with respect to the spacecraft equator.

Is the apparent Earth disk lit, and are the arcs ϵ and ϕ_0 within specified limits?

Does at least one of the two points (one per slit) of contact of the fan beam with the Earth horizon belong to a *lit limb*? This is a nontrivial question that was presumably overlooked in past operations. We will briefly outline how to get the relevant equations, both for the meridian as well as for the skew slit. To translate this question into geometry, we first refer to Fig. 1, with the plane defined by S, E, and A. This plane, in turn, is the zero reference for the angle $\pm\phi_0$, which is described in Fig. 3. This angle, $2\phi_0$, is in fact a dihedral angle around the line $\overline{\mathrm{AE}}$ and centered around the arc γ belonging to the SEA plane. This means that the limits of the crescent we are considering form a dihedral angle around $\overline{\mathrm{AE}}$ bound by $\tau + \phi_0$ and $\tau - \phi_0$ or $\pi - \tau \pm \phi_0$, measured from the meridian NE, and where τ is defined in Fig. 1. Limiting ourselves first to the meridian slit, we have to compute the dihedral angle $\widehat{\mathrm{T_aEN}} = \psi_m$ in Fig. 5 with the plane NAE to see whether it falls inside the $\pm\phi_0$ interval around the plane SAE. We obtain

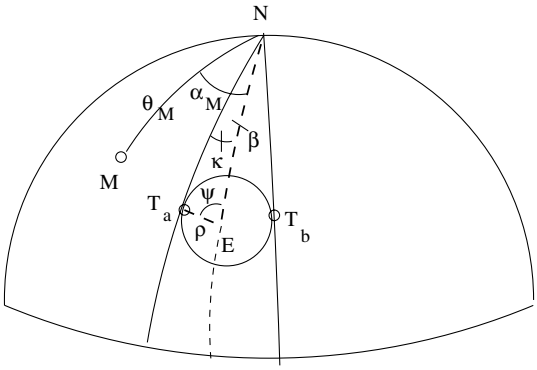

Fig. 5 Earth tangency by the meridian slit.

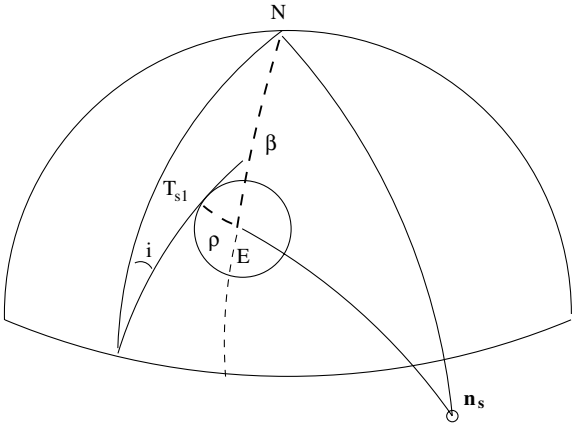

Fig. 6 Earth tangency by the skew slit.

$$\cos\kappa = \sin\psi_m \cos\rho \tag{27}$$

for both the space/Earth and Earth/space contact points.

For the skew slit, the point of tangency T_{s1} at space/Earth is shown in Fig. 6, where n_s corresponds to the position of the skew slit normal on the unit sphere at the instant of contact. We now consider the spherical triangle NEn_s and note that $\widehat{Nn_s} = \pi/2 + i$ and $\widehat{En_s} = \pi/2 - \rho$. The angles ρ and i are known as well as β, because we are dealing with a coverage prediction problem. Consequently, a simple application of the cosine rule immediately yields

$$\cos\psi_{s1} = \frac{\sin\rho\cos\beta + \sin i}{\cos\rho\sin\beta} \tag{28}$$

For space/Earth, on the one hand, we ask whether or not

$$\tau - \phi_0 + \sigma < \psi < \tau + \phi_0 - \sigma$$

and for Earth/space, on the other hand, we check if

$$\pi - \tau - \phi_0 + \sigma < \psi < \pi - \tau + \phi_0 - \sigma$$

is satisfied. The computation of ψ_{s2} for the Earth/space case is left to the reader.

The blinding of the FBAS by the sun or the disturbance by the moon is the last question to clear. Referring to Fig. 1, we have sun blinding of the meridian slit if the angle α is either small or close to 2π. Normally in this case, the satellite is on the dark side of the Earth, and we can assume that this is no problem. For the moon, things are different, because repeated disturbances will occur each time the moon (not eclipsed by the Earth relative to the spacecraft position) crosses a slit field of view more or less at the same instant as a limb crossing with a lit Earth lune, thereby corrupting the electronically assumed illumination gradient. In Fig. 5, this happens when the moon direction **M** crosses either the meridian NT_a or NT_b. To translate this occurrence into trigonometry, we note that the triangle MNE (to be included in Fig. 5) is, in principle, equal to the triangle SNE displayed in Fig. 1, after replacing **S** by **M**, giving rise to the moon colatitude θ_M and the moon–Earth dihedral angle α_M. To not suffer from moon interference by the meridian slit, the conditions

$$\sigma < |\alpha + \kappa - \alpha_M|$$

and

$$\sigma < |\alpha - \kappa - \alpha_M|$$

shall be satisfied separately. If ρ_M is the apparent angular radius of the moon, we can employ the condition that the skew slit crosses the moon direction, or

$$(\mathbf{n_s}, \mathbf{M}) = \pm\sin\rho_M \tag{29}$$

and this point shall not coincide with $(\mathbf{n_s}, \mathbf{E}) = \pm\sin\rho$ within a given safety margin σ. The moon corruption does not prevent coverage as such, but it essentially may falsify the sensing time tags obtained in this situation. These moon disturbances were not included in the ground-based coverage predictions of the four satellite missions mentioned in the Introduction.

Conclusions

We assembled, unified, and complemented the technical information, partially no longer accessible, on fan beam albedo sensors, providing sections dealing with the geometrical sensor description, the generation of measurement equations, and, finally, measurement coverage prediction. The last section especially, complementing past knowledge and practice, relies on a basic but nevertheless comprehensive knowledge of attitude determination of spin-stabilized satellites and specific albedo-related geometry. This background was presented in the third, fourth, and fifth sections. Past estimation methods that had been applied to albedo sensing data are outdated by now, and a proposal was added on how to replace them.

References

[1] Wertz, J. (ed.), *Spacecraft Attitude Determination and Control*, Kluwer Academic, London, 1978.

[2] Fraiture, L., "Fan Albedo Sensor Attitude Geometry," ESA/European Space Operations Centre Orbit and Attitude Division Working Paper 354, Feb. 1988.

[3] Pallaschke, S., Munoz, I., Rodriguez-Canabal, J., Sieg, D., and Yde, J. J., "CLUSTER: Mission overview and End-of-Life Analysis," *Proceedings of 20th International Symposium on Space Flight Dynamics*, CP-214158, NASA, Annapolis, MD, Sept. 2007.

[4] Deasy, H., "Fan Albedo Sensor Geometry Application to Coverage Criteria," ESA/European Space Operations Centre Orbit and Attitude Division Working Paper 366, March 1988.

[5] Deasy, H., "Fan Beam Albedo Sensor: Error Analysis," ESA/European Space Operations Centre Orbit and Attitude Division Working Paper 373, July 1988.

[6] Fraiture, L., "Spacecraft Attitude Sensing Based on the Earth's Radiation," *ESA Bulletin*, No. 33, Feb. 1983, pp. 29–36.

[7] Fraiture, L., Wiengarn, N., and Chambaz, B., "Irregularities in the Motion of Spin Stabilized Satellites," *Proceedings of the First International Symposium on Spacecraft Flight Dynamics*, SP 160, ESA, Paris, Aug. 1981, pp. 87–104.

[8] Werking, R. D., "A Generalized Technique for Using Cones and Dihedral Angles in Attitude Determination," NASA Goddard Space Flight Center TM-X-70705, Greenbelt, MD, 1973.

[9] Johansson, L. P., *Evaluation of HEOS-1 Attitude Results*, European Space Research and Technology Centre Technical Information Center , ESA (European Space Research Organization), CR-346, 1975.

[10] Fraiture, L., "Attitude Reconstitution Filtering: Yes or No?," *Proc. of the Second International Symposium on Flight Dynamics*, SP 255, ESA, Paris, 1986, pp. 403–414.

[11] Fraiture, L., "The Information Dilution Theorem," *ESA Journal*, Vol. 10, No. 4, Dec. 1986, pp. 381–386.

[12] Fraiture, L., "Spin-Axis Attitude Estimation by a Controlled Correlation Method," *Journal of Spacecraft and Rockets*, Vol. 42, No. 1, Jan./Feb. 2005, pp. 58–65.
doi:10.2514/1.6148

[13] van der Ha, J. C., "Equal Chord Attitude Determination Method for Spinning Spacecraft," *Journal of Guidance, Control, and Dynamics*, Vol. 28, No. 5, Sept./Oct. 2005, pp. 997–1005. doi:10.2514/1.10660

[14] Fraiture, L., "Attitude Estimation with GPS-Like Measurements," *Journal of the Astronautical Sciences*, Vol. 54, Nos. 4–5, July 2006, pp. 595–617.

D. Spencer
Associate Editor